GPR92 as a New $G_{12/13}$- and G_q-coupled Lysophosphatidic Acid Receptor That Increases cAMP, LPA5[*]

Chang-Wook Lee, Richard Rivera, Shannon Gardell, Adrienne E. Dubin, and Jerold Chun[1]

From the Department of Molecular Biology, Helen L. Dorris Institute for Neurological and Psychiatric Disorders, The Scripps Research Institute, La Jolla, California 92037

The signaling effects of lysophospholipids such as lysophosphatidic acid (LPA) are mediated by G protein-coupled receptors (GPCRs). There are currently four LPA receptors known as $LPA_{1–4}$. Genetic deletion studies have identified essential biological functions for LPA receptors in mice. However, these studies have also revealed phenotypes consistent with the existence of as yet unidentified receptors. Toward identifying new LPA receptors, we have screened collections of GPCR cDNAs using reverse transfection and cell-based assays. Here we report an interim result of one screen to identify receptors that produced LPA-dependent changes in cell shape: the orphan receptor GPR92 has properties of a new LPA receptor. Sequence analyses of human GPR92 and its mouse homolog have ~35% amino acid identity with LPA_4/GPR23. The same cell-based approaches that were used to identify and/or characterize $LPA_{1–4}$, particularly heterologous expression in B103 cells or RH7777 cells, were utilized and compared with known LPA receptors. Retroviral-mediated expression of epitope-tagged receptors was further combined with G protein minigenes and pharmacological intervention, along with calcium imaging and whole-cell patch clamp electrophysiology. LPA-dependent receptor internalization following exposure to LPA but not related lysophospholipids was observed. Furthermore, LPA induced concentration-dependent activation of $G_{12/13}$ and G_q and increased cAMP levels. Specific [3H]LPA binding was detected in cell membranes heterologously expressing GPR92 but not control membranes. Northern blot and reverse transcriptase-PCR studies indicated a broad low level of expression in many tissues including embryonic brain and enrichment in small intestine and sensory dorsal root ganglia, as well as embryonic stem cells. These results support GPR92 as a fifth LPA receptor, LPA5, which likely has distinct physiological functions in view of its expression pattern.

Lysophosphatidic acid (LPA)[2] is a lysophospholipid whose functions are mediated by at least four G protein-coupled receptors (GPCRs) referred to as $LPA_{1–4}$ (1–4). These receptors couple to multiple G proteins, particularly $G_{12/13}$, G_i, and G_q, and possibly G_s. In turn, activated downstream pathways are even more diverse and include stimulation of phospholipase C and D, inhibition of adenylyl cyclase (5, 6), and stimulation of small GTPases, mitogen-activated protein kinases, and phosphoinositide 3-kinase (7, 8). Receptor-mediated actions of LPA have important influences on cell survival, cytoskeletal remodeling, cell migration, and cell proliferation (5, 9–11).

LPA signaling via GPCRs has physiological consequences that have been revealed through gene deletion studies of most of the LPA receptors (12, 13). This approach has identified roles in normal organismal development, nervous system development, influences on brain architecture and function (12, 14, 15), female fertility and implantation (16), and the initiation of neuropathic pain (17). While essential roles for individual receptors have been observed, it has been somewhat surprising that more profound effects like early embryonic lethality have not been seen from single or even double receptor knock-outs (13), particularly in view of deletion studies for a key LPA biosynthetic enzyme, autotaxin, that produces complete embryonic lethality (18).

To identify possible new LPA receptors, we have used reverse transfection (19) in an unbiased screening approach. Reverse transfection utilizes a strategy whereby collections of cDNAs are arrayed on slides or in tissue culture wells followed by placement of a single, suitable cell line that can 1) take up and express the cDNA in question and 2) provide a reliable readout. During the initial phases of one screen to identify LPA-dependent changes in the actin cytoskeleton, a positive response was observed for the orphan GPCR known as GPR92. Here we report the initial characterization of this novel LPA receptor and describe downstream signaling pathways mediated by LPA activation of GPR92.

EXPERIMENTAL PROCEDURES

Materials—LPA (1-oleoyl-2-hydroxy-*sn*-glycero-3-phosphate) was purchased from Avanti Polar-Lipids (Alabaster, AL). Y27632 and pertussis toxin (PTX) were obtained from Calbiochem (La Jolla, CA). B103 neuroblastoma cells and RH7777 hepatoma cells were from laboratory stocks as reported previously. Retrovirus expression vector (LZRS-EGFP) and Phoenix retrovirus producer cell lines were provided by Dr. Garry P. Nolan (Stanford University, Stanford, CA). The initial GPCR collection was obtained through the IMAGE consortium and Dr. Mike Brownstein (National Institutes of Health/NIMH; image.llnl.gov) and combined with additional cDNA clones produced by standard PCR

[1] To whom correspondence should be addressed: Dept. of Molecular Biology, The Scripps Research Institute, 10550 North Torrey Pines Rd., ICND-118, La Jolla, CA 92037. Tel.: 858-784-8410; Fax: 858-784-7084; E-mail: jchun@scripps.edu.
[2] The abbreviations used are: LPA, lysophosphatidic acid; GPCR, G protein-coupled receptor; PTX, pertussis toxin; HA, hemagglutinin; EGFP, enhanced green fluorescent protein; BSA, bovine serum albumin; PBS, phosphate-buffered saline; BAPTA, 1,2-bis(2-aminophenoxy)ethane-N,N,N',N'-tetraacetic acid; ANOVA, analysis of variance; S1P, sphingosine 1-phosphate.

and cDNA library screening approaches. [³H]LPA (1-oleoyl-[9,10-³H]LPA, 47 Ci/mmol) was obtained from PerkinElmer Life Sciences. Ki16425 (3-(4-[4-([1-(2-chlorophenyl)ethoxy]carbonylamino)-3-methyl-5-isoxazolyl]benzylsulfonyl)propanoic acid) was a gift from Kirin Brewery Co. (Takasaki, Japan).

Protein Sequence Alignment and Construction of the Phylogenetic Tree—Protein sequences of GPCRs were obtained from GenBank™ and Swiss-Prot. The amino acid alignment and phylogenetic tree were assembled using the computer programs ClutalW and TreeTop.

Cell Culture and Stable Transfection—B103 cells and RH7777 cells were maintained in Dulbecco's modified Eagle's medium with 10% heat-inactivated fetal bovine serum (Hyclone, Logan, UT) and antibiotics. For experiments, cells were serum-starved overnight before examination. To produce stable cell lines, B103 cells were transfected with linearized HA-tagged GPR92-pcDNA3.1 (Invitrogen) using Effectene transfection reagent (Qiagen, Valencia, CA) and stable transfectants selected using 1 mg/ml of geneticin (Invitrogen).

Construction of Retroviral Vectors and Production of Retroviruses for LPA_1, GPR92, and G Protein Minigenes—Retrovirus for mouse LPA_1 was produced as described (20). For GPR92, an epitope HA tag was introduced onto the 5′ end of the of a full-length human GPR92 cDNA by PCR using the following primers: 5′-GAATTCACCATGTACCCATACGATGT-TCCAGATTACGCTTTAGCCAACAGCTCCTCAACC-3′ (forward) and 5′-GAATTCTCAGAGGGCGGAATCCTG-3′ (reverse). The cDNA was amplified using the Expand High Fidelity PCR system (Roche Applied Science, Mannheim, Germany). PCR products were then gel-purified using QiaexII gel extraction kit (Qiagen, Valencia, CA) and subcloned into the pGEM-T Easy T vector (Promega, Madison, WI). The cDNA insert was sequenced at the Scripps Research Insitute sequencing core facility and validated sequences subsequently cloned into the EcoRI site of the LZRS-EGFP Moloney murine leukemia retroviral vector. Retrovirus was produced by transfection of the Phoenix ecotropic packaging cell line (21) using FuGENE 6 transfection reagent (Roche Diagnostics). Retroviral supernatant was harvested 48 h post-transfection, filtered through a 0.45- μm filter, aliquoted, and frozen. For G protein minigenes, $G_{q/11}$ (MGLQLNLKEYNLV), G_s (MGQRMHLRQYELL), G_{12} (MGLQENLKDIMLQ), and G_{13} (MGLHDNLKQLMLQ) were constructed as described (22) and subcloned into the above retroviral vector.

Reverse Transfection of GPCR Collection—Reverse transfection method was performed as published (19). Briefly, for each cDNA, 0.3 μg of DNA (encoding GPCR and EGFP in a 10 to 1 ratio) was mixed with 5 μl of Effectene (Qiagen), then mixed with 7.5 μl of 0.05% gelatin (Sigma, Type B, St. Louis, MO) and used to coat the bottom of a multiwell plate. After drying, B103 cells were seeded for reverse transfection and EGFP-positive cells analyzed for LPA-dependent neurite retraction using a fluorescence microscope (Axio Imager D1, Carl Zeiss, Thornwood, NY).

Reverse Transcriptase-Polymerase Chain Reaction—RNA was extracted from cultured cells or tissues using TRIzol reagent (Invitrogen) as described in the manual. Total RNA (5 μg) was reverse-transcribed for 50 min at 42 °C using Superscript II

reverse transcriptase (Invitrogen). An equal aliquot of cDNA was used to amplify the different receptor transcripts using the following conditions: 94 °C for 30 s, 60 °C for 45 s, and 72 °C for 45 s for a total of 30–35 cycles. The primers were used as follows: GPR92, 5′-AGGAAGAGCAACCAAGCA-CAG-3′ (forward for B103 and RH7777), 5′-AGGAAGAGCA-ACCGATCACAG-3′ (forward for mouse tissues), and 5′-ACCACCATATGCAAACGATGTG-3′ (reverse for both cell lines and tissues); β-actin, 5′-TGGAATCCTGTGGCATCCA-TGAAAC-3′ (forward) and 5′-TAAAACGCAGCTCAGTAA-CAGTCCG-3′ (reverse). A hot start of 5 min at 94 °C and a final incubation of 10 min at 72 °C were carried out for all PCR reactions. The PCR products were separated by electrophoresis on a 1.2% agarose gel.

LPA Binding Assay—LPA binding was performed as described previously (23). Cells were harvested, homogenized in ice-cold binding buffer (20 mM Tris-HCl, pH 7.5) containing 1 mM EDTA and protease inhibitor mixture (Roche Diagnostics) and centrifuged at 2,000 rpm for 10 min at 4 °C. The supernatant was centrifuged further at 15,000 rpm for 30 min at 4 °C. The membrane preparation (30 μg) was incubated with 20 nM [³H]LPA (1-oleoyl-[9,10-³H]LPA, 47 Ci/mmol) in LPA binding buffer containing 0.1% fatty acid-free BSA (Sigma) and 0.5 mM $CuSO_4$ for 30 min at room temperature, and the bound [³H]LPA was collected onto a Unifilter 96-GF/B (PerkinElmer Life Sciences). The filter was then rinsed 10 times with binding buffer containing 1% normal BSA and dried for 30 min at 50 °C. After the addition of 30 μl of MicroScint-O (PerkinElmer Life Sciences) to each well of the filter, radioactivity was measured using a microplate liquid scintillation counter. Total and nonspecific binding was evaluated in the absence and presence of 10 μM unlabeled LPA, respectively.

Membrane Fractionation and Western Blotting—Cells were homogenized on ice, using a Dounce homogenizer, in homogenization buffer (20 mM Tris buffer, pH 7.5) containing 1 mM EGTA, 1 mM EDTA, and protease inhibitor mixture (Roche Diagnostics). The homogenized sample was first cleared at 2,000 rpm for 5 min at 4 °C, and the supernatant was further centrifuged at 15,000 rpm for 90 min. The pellets were resuspended on ice in the homogenization buffer containing 1% Triton X-100. The extracted pellets were centrifuged at 15,000 rpm for 20 min, and the obtained supernatant membrane fraction was separated under reducing, denaturing conditions on a 4–12% SDS-polyacrylamide gel (Invitrogen) and transferred to a polyvinylidene difluoride membrane (Millipore, Woburn, MA). The HA-tagged proteins were detected with an anti-HA antibody (Roche Diagnostics), horseradish peroxidase-conjugated anti-mouse secondary antibody, and visualized with ECL Plus (Amersham Biosciences).

Immunofluorescence and Receptor Internalization Assay—Cells were plated on poly-L-lysine-coated glass coverslips in 24-well plates. After stimulation with LPA, cells were fixed with 4% paraformaldehyde/PBS, permeabilized with 0.1% Triton X-100/PBS for 15 min, and blocked with 3% BSA/PBS for 30 min. F-actin was detected with 25 μg/ml rhodamine-phalloidin (Sigma) in PBS, 1% BSA for 40 min. Samples were visualized on a fluorescence microscope (Carl Zeiss). For the internalization

FIGURE 1. **Predicted amino acid alignment of the human and mouse LPA₄/GPR23 and GPR92 proteins and phylogenetic tree of the human LPA and S1P receptors.** *A*, alignment of the amino acid sequences created using the ClustalW multiple sequence alignment program, "*" means identical, ":" and "." means conserved and semiconserved substitution, respectively. *B*, phylogenetic tree showing protein sequence relationship of the human LPA and S1P receptor families. The *x* axis values are a ruler that indicates the lengths of the horizontal branches. The amino acid sequence divergence between any pair of sequences is equal to the sum of the lengths of the horizontal branches. Shorter lengths mean more closely related genes.

assay, serum-starved cells (12–16 h) were treated with BSA or LPA, or sphingosine 1-phosphate (S1P), and then fixed with 4% paraformaldehyde in PBS for 1 h and permeabilized with 0.1% (w/v) Triton X-100 with 3% BSA in PBS. HA-tagged receptor was detected using an anti-HA antibody and Cy3-conjugated anti-mouse IgG antibody (Jackson ImmunoResearch Laboratories, West Grove, PA). The cells were analyzed using standard and confocal fluorescence microscopy (Carl Zeiss).

cAMP Measurements—B103 cells were serum-starved on 24-well plates with or without PTX (200 ng/ml) overnight. After treatment with 0.5 mM 3-isobutyl-1-methylxanthine for 20 min, cells were stimulated for 30 min with or without forskolin (5 μM) using a range of LPA concentrations. The cells were lysed with 0.1 N HCl, and then cellular cAMP levels were measured using an enzyme-linked immunosorbent assay-based detection kit (Cayman Chemicals, Ann Arbor, MI) according to the manufacturer's directions.

Imaging of Intracellular Calcium Levels—Cells were plated on glass coverslips, loaded with Fura-2 acetoxymethyl ester (2.5 μM), and incubated for 30–60 min at 37 °C in 1.5 μM pluronic acid (Molecular Probes, Eugene, OR) in Opti-MEM (Invitrogen). Cells were then washed with Opti-MEM. Coverslips were placed in a laminar flow perfusion chamber (Warner Instrument Corp., Hamden, CT) and constantly perfused with Opti-MEM, LPA (1 μM) or ionomycin (1 μg/ml, Calbiochem) was bath-applied. Images of Fura-2-loaded cells with the excitation wavelength alternating between 340 and 380 nm were captured with a cooled CCD camera. Following subtraction of background fluorescence, the ratio of fluorescence intensity at the two wavelengths was calculated. Ratio levels in groups of 20–40 individual cells were analyzed using MetaFluor (Universal Imaging Corp., West Chester, PA).

Electrophysiology—Whole cell patch clamp technique was used to record from B103 cells, 2–3 days

FIGURE 2. **Surface expression and LPA-induced receptor internalization of GPR92.** *A*, schematic of GPR92-retroviral expression construct. *LTR*, long terminal repeat; ψ, retrovirus packaging signal; *IRES*, internal ribosome entry site. *B*, detection of endogenous GPR92 expression in B103 cells and RH7777 cells by RT-PCR. RNA was isolated from GPR92-transfected or non-transfected B103 cells or RH7777 cells and reverse-transcribed. Fragments of cDNAs were amplified using specific primers as described under "Experimental Procedures." *C*, Western blot analysis of the membrane fraction isolated from B103 cells infected with the empty vector (SOO3) or HA-GPR92 retroviruses. *D*, HA-tagged GPR92 expressing cells labeled with Cy3-conjugated antibody. The labeling shows cell surface (*arrowheads*) and internalized receptor signal (*arrow*) after treatment with 0.1% fatty acid-free BSA, LPA (1 μM), or S1P (1 μM) for 15 min. The images were acquired using confocal microscopy. EGFP indicates GPR92 retrovirus-infected cells. *E*, [³H]LPA binding to plasma membranes isolated from GPR92-expressing B103 cells. [³H]LPA (4,042 dpm) was incubated with 30 μg of membrane fraction for 30 min at room temperature. Excess unlabeled LPA (10 μM) was used to determine nonspecific binding. The specific binding was calculated by subtracting the nonspecific binding from the total binding value. Total binding values were 369 ± 60 dpm (pcDNA3.1) and 666 ± 44 (GPR92), nonspecific binding values were 282 ± 26 and 325 ± 24, while specific binding values were 87 ± 37 and 341 ± 23, respectively. Data are the mean ± S.D. ($n = 3$). **, $p < 0.01$ (using Student's t test) *versus* empty vector-transfected cells.

trodes were fabricated from borosilicate capillary tubing (B150-86-10; Sutter Instrument, Novato, CA). The electrodes were coated with dental periphery wax (Miles Laboratories, South Bend, IN) and had resistances of 2–4 MΩ when containing intracellular saline (in mM): 100 potassium gluconate, 25 KCl, 3 MgCl$_2$, 0.483 CaCl$_2$, 1.0 BAPTA-K$_4$, 10 hemi-Na-HEPES, pH 7.4. Whole cell access was achieved by applying short, high voltage pulses (zap), and data were accepted if the access resistance was greater than 15 MΩ ("resistive" whole cell configuration). If the access resistance was less than 15 MΩ, only half of the GPR92-infected cells responded to LPA. The average voltage error was 8 ± 2 mV ($n = 15$) at the potentials reported. Current signals were detected and filtered at 10 KHz with a MultiClamp 700A amplifier (Molecular Devices (previously Axon Instruments), Union City, CA), digitally recorded with a Digi-Data 1322A laboratory interface (Axon Instruments) and PC-compatible computer system, and stored for off-line analysis. Data acquisition and analysis were performed with PClamp9 software (Axon Instruments). The total membrane capacitance (C_m) was determined as the difference between the maximum current after a 30 mV hyperpolarizing voltage ramp from −20 mV generated at a rate of 10 mV/ms and one-tenth of the difference between the current at the end of the ramp and the steady state current at the final potential (20 μs sampling rate) (24) was comparable with the C_m determined on-line. Stimulus-induced changes in whole cell currents were monitored using a voltage-ramp protocol. Usually, cells were held at −50 mV and V_m was stepped to −120 mV for 60 ms and ramped to +120 mV (at a rate of 1.2 mV/ms) at 0.5 Hz. All currents are normalized

to the C_m during stimulus application (current density). Ki16425 (10 μM) was bath-applied for 3 min prior to LPA exposure.

Northern Blot Analysis—A Northern blot containing 2 μg/lane of adult mouse poly(A)$^+$ RNA from several mouse tissues was

after retrovirus infection. Extracellular solution contained (in mM): 145 NaCl, 2.5 KCl, 1.5 CaCl$_2$, 1.5 MgSO$_4$, 10 HEPES, 10 dextrose, pH 7.4 (with NaOH). Compounds were added to the bath by gravity perfusion at room temperature. No effect of vehicle was observed in these experiments. Recording elec-
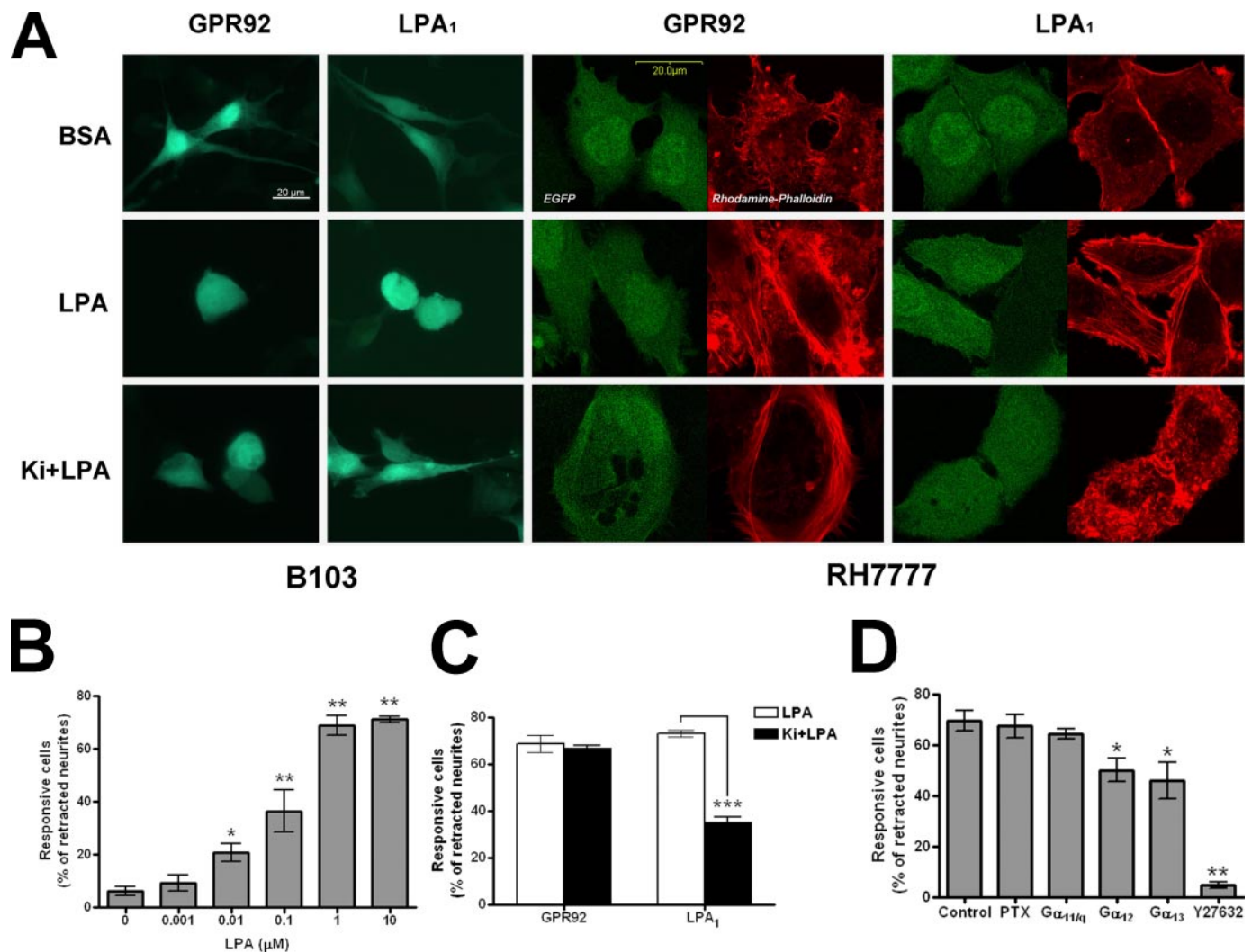
FIGURE 3. **GPR92-mediated *versus* LPA$_1$-mediated neurite retraction and stress fiber formation.** *A*, neurite retraction and stress fiber formation by GPR92 *versus* LPA$_1$. GPR92- or LPA$_1$-infected B103 cells (*left*) or RH7777 cells (*right*) were treated with 1 μM LPA, in the absence or presence of 5 μM of Ki16425 for 30 min (*bottom*). B103 cells were fixed and mounted on glass slides. RH7777 cells were fixed and stained with rhodamine-phalloidin to detect actin stress fibers. *B*, quantified results of the above B103 cell data. LPA concentration-dependent data are mean ± S.E. (*n* = 3). *, *p* < 0.05; **, *p* < 0.01 (one-way ANOVA) *versus* basal 0 μM of LPA. *C*, effect of Ki16425 exposure. Data are the mean ± S.E. (*n* = 3). ***, *p* < 0.005 (Student's *t* test). *D*, signaling responses of GPR92 expressing B103 cells following LPA exposure. GPR92-expressing B103 cells were pretreated with PTX (200 ng/ml) overnight, infected with a G protein minigene, or pretreated with Y-27632 (10 μM). Cells were stimulated with 1 μM LPA for 30 min, then fixed and counted. Data are the mean ± S.E. (*n* = 3). *, *p* < 0.05; **, *p* < 0.01 (one-way ANOVA) *versus* control.

purchased from OriGene Technologies Inc. (Rockville, MD). This Northern blot was probed with a random primed ^{32}P-labeled fragment of the mouse GPR92 cDNA. DNA labeling was performed with the random primed DNA labeling kit (Roche Diagnostics) and labeled probe, and unincorporated nucleotides were separated by passing the reaction mixture over a Sephadex G-50 quick spin column (Roche Diagnostics). The Northern blot was then probed overnight in ULTRAhyb hybridization solution (Origen) containing the labeled probe, washed several times, and analyzed using a PhosphorImager detection system.

Statistical Analysis of Data—The data are presented ± S.D. Each data point was calculated from triplicate samples unless otherwise indicated. Statistical analysis was performed by one-way ANOVA and Dunnett's method or Student's *t* test. ***, *p* < 0.001; **, *p* < 0.01; *, *p* < 0.05.

RESULTS

Comparison of amino acid sequences showed that GPR92 has ~35% amino acid identity with the LPA$_4$/GPR23 receptor. Protein sequence alignment of mouse and human GPR92 demonstrated 80% identity (Fig. 1*A*). Phylogenetic analysis indicated that GPR92 was more related to the fourth receptor LPA$_4$/GPR23 when compared with the other less similar LPA and S1P receptors (Fig. 1*B*).

The initial identification of GPR92 as a cytoskeleton-influencing LPA receptor in a reverse transfection screen was reassessed by retroviral mediated GPR92 expression. To ascertain appropriate expression of receptor protein, human GPR92 was epitope-tagged with HA at the extracellular N terminus (Fig. 2*A*), and the construct was introduced into a replication-incompetent Moloney leukemia retroviral vector to allow virus production and transduction of single-copy GPR92 expression
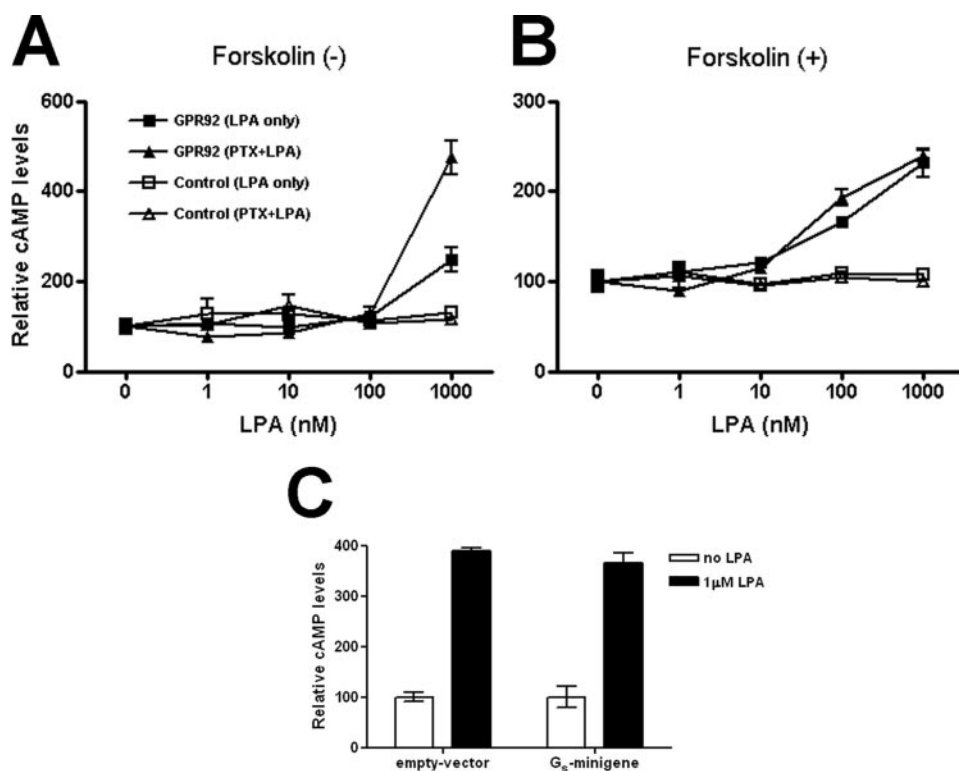
FIGURE 4. **Effects of LPA on cAMP accumulation in GPR92-expressing B103 cells.** *A*, effects of LPA on basal cAMP levels. GPR92-expressing B103 cells were stimulated with increasing concentrations of LPA in the presence of 0.5 mM 3-isobutyl-1-methylxanthine. The basal cAMP content in GPR92-expressing cells (■), PTX-treated cells (200 ng/ml) (▲), and empty vector transfected cells (□, PTX-untreated cells; △, PTX-treated cells) are indicated. The increase in cAMP levels following PTX treatment likely results from blockade of other basally active, G_i-coupled receptors in B103 cells. *B*, effects of forskolin on cAMP accumulation. Cells were stimulated with LPA in the presence of 5 μM forskolin in the same manner as in *A*. *C*, GPR92-expressing B103 cells were infected with a control retrovirus or G_s minigene retrovirus and then cAMP assay was performed.

following cell infection. Two cell lines used throughout this study, B103 and RH7777 (23), were examined for GPR92 gene expression by PCR using intron-spanning primers for non-coding exon 1 and coding exon 2 (Fig. 2*B*). B103 cells do not express endogenous GPR92 mRNA, and it was therefore used in all subsequent analyses. Surprisingly, GPR92 mRNA was detected in RH7777 cells, further revealing two bands consistent with alternative splicing in a 5'-non-coding region of GPR92. However, no LPA-dependent responses have been observed in naïve cells from either B103 or RH7777.

HA-tagged GPR92 virus-infected *versus* control virus-infected cells were examined by Western blot analysis. Cell membrane fractions identified a single band of the expected molecular mass (Fig. 2*C*). Consistent with this result, tagged receptor could be identified on the surface of GPR92 expressing B103 cells (Fig. 2*D*) using Cy3-anti HA immunolabeling and visualized with confocal microscopy. No other known LPA receptors were up-regulated in GPR92 infected cell lines, as assessed by PCR (data not shown). GPCRs typically undergo internalization upon treatment with a full agonist (25), and heterologously expressed GPR92 was therefore assessed for LPA-dependent receptor internalization *versus* a distinct lysophopholipid, S1P. Cell surface GPR92, revealed by Cy3 immunolabeling, was internalized following LPA but not S1P exposure (Fig. 2*D*). To assess the ability of GPR92 to bind LPA, isolated membranes from B103 cells stably expressing GPR92 or control vector were

tested for specific [³H]LPA binding. Membranes derived from GPR92-expressing cells, but not control vector infected cells, revealed a statistically significant increase in specific [³H]LPA binding (Fig. 2*E*).

Positive controls in which LPA_1 had been heterologously expressed produced neurite retraction in B103 cells and stress fiber formation in RH7777 cells (Fig. 3*A*). GPR92 was identically assessed. When GPR92- or LPA_1-expressing cells were pretreated with 5 μM Ki16425 (LPA_1 and LPA_3 receptor antagonist) for 30 min, only LPA_1-mediated cellular responses were blocked, while GPR92-mediated cellular responses still remained (Fig. 3, *A* and *C*). GPR92-mediated neurite retraction of B103 cells was dependent on LPA concentration (Fig. 3*B*). Ki16425 strongly inhibited neurite retraction of LPA_1-expressing B103 cells but did not affect GPR92-expressing cells (Fig. 3).

It is well established that $G_{12/13}$ couples to LPA receptors and activates downstream RhoA to induce actin stress fiber formation as well as other RhoA-dependent cellular effects (26–28), while $G_{q/11}$-mediated signaling can also activate RhoA (28, 29). To determine which G proteins couple to GPR92, several approaches were utilized, including standard pharmacological intervention and the use of "minigenes" for defined G proteins (22) (Fig. 3*D*). We first focused on pathways that could produce changes in the cytoskeleton: G_i-mediated Rac activation (30) and $G_{12/13}$- or $G_{q/11}$-mediated Rho activation. Only blockade of $G_{12/13}$ (using G_{12} and G_{13} minigenes) and downstream Rho (using Rho kinase inhibitor, Y27632) could block neurite retraction (Fig. 3*D*). Neither PTX nor a dominant negative Rac (RacN17, data not shown) abolished LPA-induced cytoskeletal alterations in GPR92-infected cells.

We next assessed whether non-cytoskeletal changes were altered with these and other G proteins (Figs. 4–6). All lysophospholipid GPCRs influence cAMP levels (15). LPA increased intracellular cAMP levels in GPR92-expressing B103 cells either in the absence (Fig. 4*A*) or presence (Fig. 4*B*) of forskolin (5 μM). Intracellular cAMP levels can be regulated by G protein $\beta\gamma$ subunits as well as G_s α subunit (31, 32). We found that use of a G_s minigene did not block cAMP accumulation by LPA in B103 cells (Fig. 4*C*). These results suggest that GPR92-mediated intracellular cAMP production might involve $\beta\gamma$ subunits, under the employed assay conditions. Similarly, many lysophospholipid receptors also couple to G_q or G_i to raise intracellular calcium levels (2, 15). In GPR92-expressing B103 cells, LPA significantly enhanced intracellular calcium levels (Fig. 5*A*), with a response latency consistent with GPCR-mediated mechanisms. This intracellular calcium
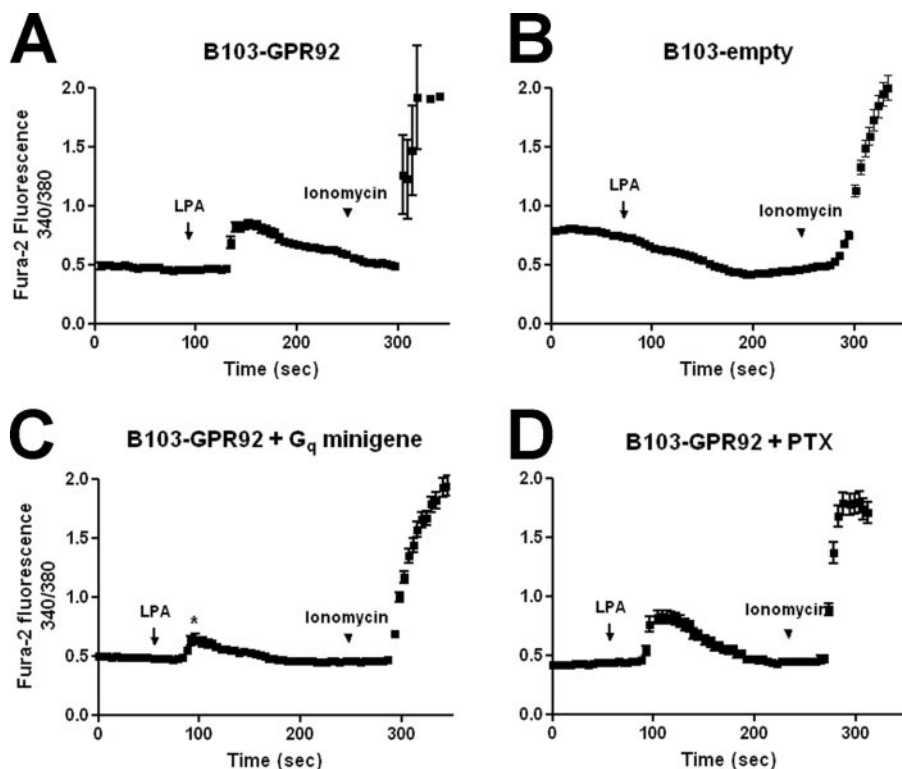
FIGURE 5. **Effects of LPA on intracellular calcium levels in GPR92-expressing B103 cells.** *A*, LPA (1 μM) increases intracellular calcium in B103 cells heterologously expressing GPR92. *B*, no effect in control cells expressing empty vector. *C*, GPR92-expressing B103 cells were infected with a G_q minigene retrovirus that attenuated calcium responses. *D*, GPR92-expressing B103 cells were treated with PTX (200 ng/ml) for 12 h, which had no effect. An *arrow* indicates the time point when LPA (1 μM) bath perfusion was initiated, and the *arrowhead* indicates the initiation of ionomycin (1 μg/ml) perfusion.
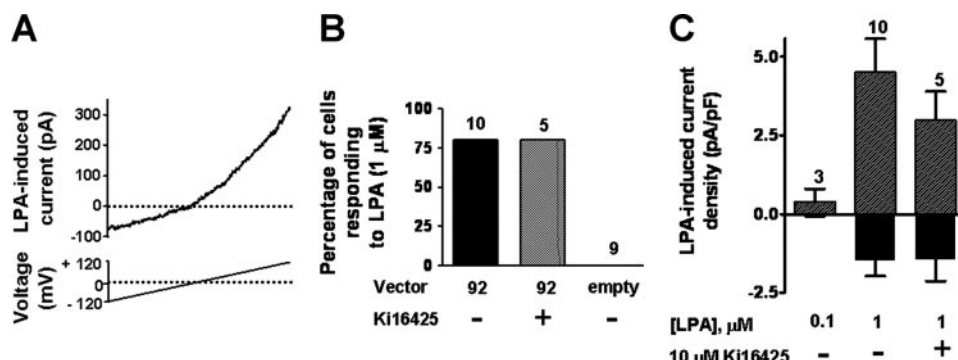
FIGURE 6. **Current evoked by LPA in GPR92-expressing cells.** *A*, LPA (1 μM) elicited an outwardly rectifying current that reversed at -7 ± 2 mV ($n = 20$ cells; mean $\pm$ S.E.). The voltage protocol is indicated below the current trace. The *dotted lines* indicate 0 current (*top*) and 0 mV (*bottom*). The latency of the response to 1 μM LPA was 34 ± 3 s ($n = 19$). *B*, the percentage of cells responding to LPA (1 μM) for cells infected with GPR92 (*bars* indicated by "*92*") and S003 vector (*bar* indicated by "*empty*") in the presence ("+") or absence ("−") of the Ki16425 compound (10 μM) is shown. The number of cells tested is shown above each *bar*. *C*, the LPA-induced current at -120 mV (negative-going bars) and $+120$ mV (positive-going bars) is shown normalized to cell capacitance (picoampere/picofarad). The response to 1 μM LPA was significantly larger than the response to 100 nM LPA ($p < 0.05$) and not significantly different from the response in the presence of 10 μM Ki16425 for values determined at $+120$ mV and -120 mV. Cells were exposed to 10 μM Ki16425 for 3 min prior to addition of LPA in the presence of Ki16425. The number of cells tested in each condition is indicated above the bars. There was no effect of LPA in the presence of Ki16425 on cells infected with vector only (data not shown).

increase was significantly blocked by expression of a G_q minigene (18 of 27 cells were completely blocked, Fig. 5*C*). However, PTX had no effect on calcium levels (Fig. 5*D*). These results indicate that GPR92 couples to G_q.

To further investigate intracellular signaling pathways modulated by GPR92 receptor activation, we used the whole cell patch clamp technique to determine whether LPA could influence ion channel function in B103 cells expressing GPR92. LPA (1 μM) activated an apparent nonselective cation conductance (Fig. 6*A*) in GPR92-infected cells ("*92*") but not cells infected with vector alone ("*empty*") (Fig. 6*B*). Preincubation of GPR92 expressing cells with the LPA$_{1/3}$ antagonist Ki16425 (10 μM) had no statistically significant effect on either the percentage of LPA responsive cells (Fig. 6*B*) or LPA-induced current density measured at either -120 (*downward bars*) or $+120$ (*upward bars*) mV (Fig. 6*C*). Currents induced by GPR92 receptor activation were outwardly rectifying (current density was greater at $+120$ mV *versus* -120 mV) and were concentration-dependent (0.1 *versus* 1 μM; Fig. 6*C*).

The expression pattern of GPR92 was assessed by Northern blot analysis on poly(A)$^+$ mRNA from adult mouse tissues probed with a fragment of the GPR92 mouse cDNA (Fig. 7*A*). Consistent with our PCR results of these and other tissues (Fig. 7*B*), GPR92 mRNA is expressed broadly at low levels, such as embryonic brain, and comparatively high levels in small intestine, and moderate levels in skin, spleen, stomach, thymus, lung, and liver. Two bands, 3.3 and 2.8 kb, were also observed by Northern analysis, consistent with RT-PCR data (Fig. 2*B*), along with a larger band (6 kb) that may represent unspliced mRNA. RT-PCR also detected signals in small subpopulations of cells that could not be assessed by Northern blot, most notably the dorsal root ganglia (*DRG*) as well as embryonic stem cells (*ES*) (Fig. 7*B*).

DISCUSSION

Lysophospholipid signaling mediated by GPCRs accounts for an expanding repertoire of organismal influences. The identification of LPA$_4$ (4) as a receptor with lower homology to other LPA GPCRs (Fig. 1) suggests that other dissimilar LPA GPCRs could well exist, as speculated previously (15). This perhaps surprising heterogeneity of LPA receptors is nonetheless consistent with previously identified heterogeneity in another class of lipid receptors, leukotriene

A
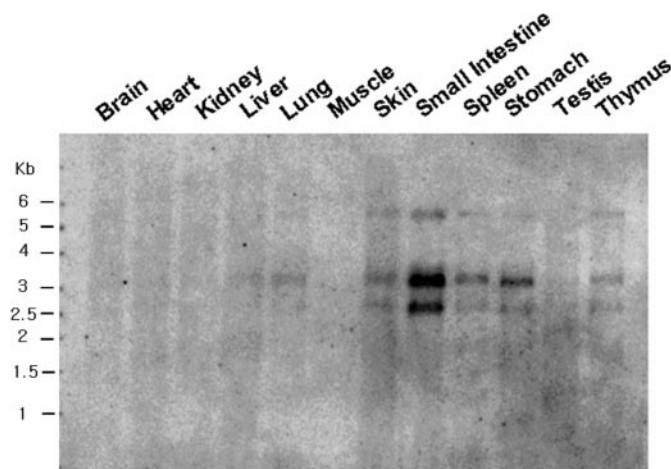
B
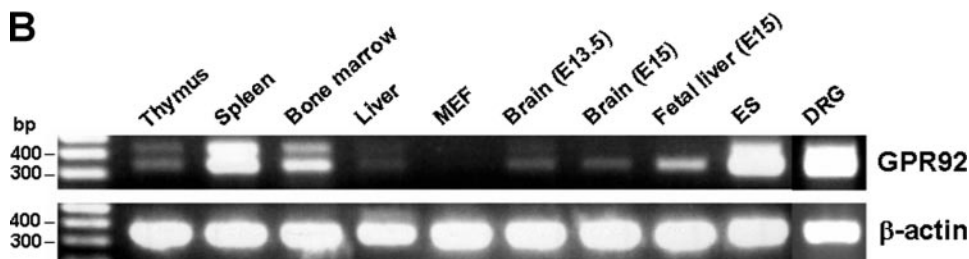
FIGURE 7. Northern blot analysis of GPR92 expression in mouse tissues. *A*, tissue poly(A)+ RNA from 6–8-week-old BALB/c adult mice: brain, heart, kidney, liver, lung, muscle, skin, small intestine, spleen, stomach, testis, and thymus. A random primed ^{32}P-labeled probe was used as described under "Experimental Procedures." *B*, total RNAs from thymus, spleen, bone marrow, liver, mouse embryonic fibroblast (*MEF*) cells, brain (E13.5), brain (E15), fetal liver (E15), embryonic stem (*ES*) cells, and dosal root ganglia (*DRG*) were assessed by RT-PCR with specific primers as described under "Experimental Procedures." β-Actin was used as a loading control.
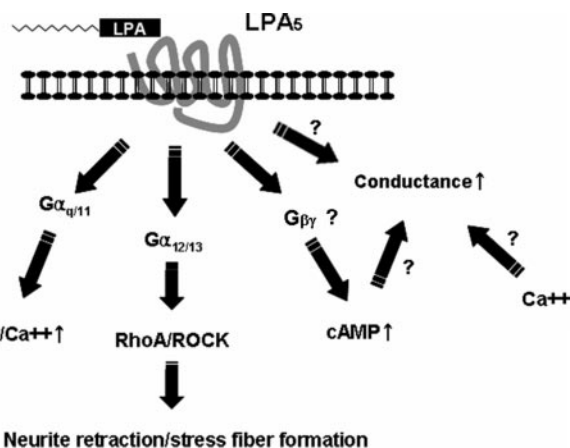
FIGURE 8. Schematic for LPA$_5$ signaling. A fifth LPA receptor, LPA$_5$, signaling increases intracellular calcium, neurite retraction, and stress fiber formation, and intracellular cAMP accumulation probably through $G_{q/11}$, $G_{12/13}$, and G protein βγ subunits, respectively. The identity of G proteins that mediate conductance changes is not known.

GPCRs (33). Using a DNA sequence-unbiased approach that focused on LPA-dependent cellular morphological changes produced by expression of putative orphan GPCRs, GPR92 was found to have attributes of previously described LPA GPCRs by conferring LPA responsivity following heterologous expression in B103 cells: 1) concentration-dependent neurite retraction mediated by $G_{12/13}$ and Rho, 2) receptor internalization, 3) increased LPA binding, 4) increased cAMP accumulation, 5) intracellular calcium mobilization, which is mediated by G_q, and 6) evoked electrophysiological currents. In addition, GPR92 expression produces LPA-dependent actin stress fibers in RH7777 cells that, while expressing mRNA for GPR92, do not respond to LPA in the absence of $G_{12/13}$-coupled LPA receptors (23). Discordant mRNA and protein expression may explain the lack of LPA responsivity in RH7777 cells that has been well documented in other systems (34–37). Taken together, the data presented here are entirely consistent with GPR92 encoding a new LPA receptor, and we therefore propose its designation as LPA$_5$ (Fig. 8).

The approaches used to make this identity have been validated over the last decade in multiple laboratories (2–4, 23, 38). With the exception of the most recently identified receptor LPA$_4$, the initial receptor identities were subsequently confirmed by independent assays including genetic deletion of one or more receptors that abolishes expected LPA signaling (12, 13, 16, 39). Heterologous expression of all five LPA receptors produces increased specific binding of [^{3}H]LPA to membrane fractions, although quantitative assessment via classical receptor-ligand binding approaches has been met with varied success that may be receptor-dependent (1, 4, 23). In the present study, saturable LPA-receptor binding could not be achieved in biologically relevant ranges, similar to previous studies, and therefore a precise K_d was not established. By contrast, the EC$_{50}$ for neurite retraction (Fig. 3) approximates the single-digit nanomolar concentrations observed previously in this assay for LPA$_1$ (1, 20, 40), indicating that LPA$_5$ is likely to be a high affinity LPA receptor, comparable with those previously identified. No attempt was made in this initial study to examine other forms of LPA beyond the 1-oleyl species used. What can be said is that the LPA$_1$- and LPA$_3$-specific antagonist Ki16425 (41) had no effect on LPA$_5$ at concentrations that block these two other receptors, indicating the probability of ligand-receptor selectivity, as expected from the distinct amino acid sequence of LPA$_5$.

LPA$_5$ complements the four previously identified GPCRs that mediate the signaling effects of LPA. While still clearly within the superfamily of GPCRs, GPR92 is notable compared with the four previously identified LPA receptors in sharing at most 35% sequence identity with LPA$_4$ and lower identities compared with LPA$_{1–3}$. Its expression pattern by Northern blot analysis is also distinct, albeit overlapping with one or more other LPA receptor genes, which suggests that LPA$_5$ will have both distinguishable functions *in vivo* and within single tissues,

at least based on its ability to increase cAMP levels, which contrasts with G_i coupling observed for LPA_{1-3}, and complements the G_s signaling of LPA_4 (4). In view of the role of LPA_1 in the initiation of neuropathic pain in an animal model (17), LPA_5 expression was examined in the peripheral nervous system and was found to be expressed in dorsal root ganglia, suggesting that it too might contribute to this disease process. Similarly, its expression in other adult tissues supports LPA_5-mediated signaling as relevant to normal function, most likely in concert with previously identified receptors, although receptor expression at the level of single cell types remains to be determined. The gene expression of LPA_5 in embryonic stem cells extends its possible roles into development and stem cell functions.

With confirmation, LPA_5 would bring the number of LPA receptors to five, complementing the five S1P receptors previously identified, all of which are GPCRs (42–44). A range of biological and medicinal roles for these receptors is emerging (45, 46), and the existence of receptors with diverse amino acid composition that recognize a common ligand portends an even richer biological and chemical landscape toward understanding and manipulating this signaling system. As lysophospholipid receptors expand into evolutionarily distinct genes, it would not be surprising to encounter additional receptors for LPA and other lysophospholipids.

Addendum—During review of this manuscript, Kotarsky *et al.* (Kotarsky, K., Boketoft, A., Bristulf, J., Nilsson, N. E., Norberg, A., Hansson, S., Sillard, R., Owman, C., Leeb-Lundberg, F. L., and Olde, B. (2006) *J. Pharmacol. Exp. Ther.* **318,** 619–628) reported that GPR92 functions as an LPA receptor.

REFERENCES

1. Hecht, J. H., Weiner, J. A., Post, S. R., and Chun, J. (1996) *J. Cell Biol.* **135,** 1071–1083
2. An, S., Bleu, T., Hallmark, O. G., and Goetzl, E. J. (1998) *J. Biol. Chem.* **273,** 7906–7910
3. Bandoh, K., Aoki, J., Hosono, H., Kobayashi, S., Kobayashi, T., Murakami-Murofushi, K., Tsujimoto, M., Arai, H., and Inoue, K. (1999) *J. Biol. Chem.* **274,** 27776–27785
4. Noguchi, K., Ishii, S., and Shimizu, T. (2003) *J. Biol. Chem.* **278,** 25600–25606
5. van Corven, E. J., Groenink, A., Jalink, K., Eichholtz, T., and Moolenaar, W. H. (1989) *Cell* **59,** 45–54
6. van der Bend, R. L., de Widt, J., van Corven, E. J., Moolenaar, W. H., and van Blitterswijk, W. J. (1992) *Biochem. J.* **285,** 235–240
7. Moolenaar, W. H. (1995) *J. Biol. Chem.* **270,** 12949–12952
8. Moolenaar, W. H., Kranenburg, O., Postma, F. R., and Zondag, G. C. (1997) *Curr. Opin. Cell Biol.* **9,** 168–173
9. Ye, X., Ishii, I., Kingsbury, M. A., and Chun, J. (2002) *Biochim. Biophys. Acta* **1585,** 108–113
10. Amano, M., Chihara, K., Kimura, K., Fukata, Y., Nakamura, N., Matsuura, Y., and Kaibuchi, K. (1997) *Science* **275,** 1308–1311
11. Fukushima, N., Weiner, J. A., Kaushal, D., Contos, J. J., Rehen, S. K., Kingsbury, M. A., Kim, K. Y., and Chun, J. (2002) *Mol. Cell Neurosci.* **20,** 271–282
12. Contos, J. J., Fukushima, N., Weiner, J. A., Kaushal, D., and Chun, J. (2000) *Proc. Natl. Acad. Sci. U. S. A.* **97,** 13384–13389
13. Contos, J. J., Ishii, I., Fukushima, N., Kingsbury, M. A., Ye, X., Kawamura, S., Brown, J. H., and Chun, J. (2002) *Mol. Cell. Biol.* **22,** 6921–6929
14. Fukushima, N., Ishii, I., Contos, J. J., Weiner, J. A., and Chun, J. (2001) *Annu. Rev. Pharmacol. Toxicol.* **41,** 507–534
15. Ishii, I., Fukushima, N., Ye, X., and Chun, J. (2004) *Annu. Rev. Biochem.* **73,** 321–354
16. Ye, X., Hama, K., Contos, J. J., Anliker, B., Inoue, A., Skinner, M. K., Suzuki, H., Amano, T., Kennedy, G., Arai, H., Aoki, J., and Chun, J. (2005) *Nature* **435,** 104–108
17. Inoue, M., Rashid, M. H., Fujita, R., Contos, J. J., Chun, J., and Ueda, H. (2004) *Nat. Med.* **10,** 712–718
18. van Meeteren, L. A., Ruurs, P., Stortelers, C., Bouwman, P., van Rooijen, M. A., Pradere, J. P., Pettit, T. R., Wakelam, M. J., Saulnier-Blache, J. S., Mummery, C. L., Moolenaar, W. H., and Jonkers, J. (2006) *Mol. Cell. Biol.* **26,** 5015–5022
19. Ziauddin, J., and Sabatini, D. M. (2001) *Nature* **411,** 107–110
20. Ishii, I., Contos, J. J., Fukushima, N., and Chun, J. (2000) *Mol. Pharmacol.* **58,** 895–902
21. Pear, W., Scott, M., and Nolan, G. (1997) *Methods in Molecular Medicne: Gene Therapy Protocols*, pp. 41–57, Humana Press, Totowa, NJ
22. Gilchrist, A., Li, A., and Hamm, H. E. (2002) *Sci. STKE.* **2002,** PL1
23. Fukushima, N., Kimura, Y., and Chun, J. (1998) *Proc. Natl. Acad. Sci. U. S. A.* **95,** 6151–6156
24. Dubin, A. E., Bahnson, T., Weiner, J. A., Fukushima, N., and Chun, J. (1999) *J Neurosci.* **19,** 1371–1381
25. Ferguson, S. S. (2001) *Pharmacol. Rev.* **53,** 1–24
26. Buhl, A. M., Johnson, N. L., Dhanasekaran, N., and Johnson, G. L. (1995) *J. Biol. Chem.* **270,** 24631–24634
27. Riobo, N. A., and Manning, D. R. (2005) *Trends Pharmacol. Sci.* **26,** 146–154
28. Wettschureck, N., and Offermanns, S. (2005) *Physiol. Rev.* **85,** 1159–1204
29. Vogt, S., Grosse, R., Schultz, G., and Offermanns, S. (2003) *J. Biol. Chem.* **278,** 28743–28749
30. Ueda, H., Morishita, R., Yamauchi, J., Itoh, H., Kato, K., and Asano, T. (2001) *J. Biol. Chem.* **276,** 6846–6852
31. Tang, W. J., and Gilman, A. G. (1991) *Science* **254,** 1500–1503
32. Federman, A. D., Conklin, B. R., Schrader, K. A., Reed, R. R., and Bourne, H. R. (1992) *Nature* **356,** 159–161
33. Brink, C., Dahlen, S. E., Drazen, J., Evans, J. F., Hay, D. W., Nicosia, S., Serhan, C. N., Shimizu, T., and Yokomizo, T. (2003) *Pharmacol. Rev.* **55,** 195–227
34. Chen, G., Gharib, T. G., Huang, C. C., Taylor, J. M., Misek, D. E., Kardia, S. L., Giordano, T. J., Iannettoni, M. D., Orringer, M. B., Hanash, S. M., and Beer, D. G. (2002) *Mol. Cell. Proteomics* **1,** 304–313
35. Dolecki, G. J., Rogers, M., and Lefkowith, J. B. (1995) *Prostaglandins* **49,** 397–414
36. Huang, Q. S., Valyi-Nagy, T., Kesari, S., and Fraser, N. W. (1997) *Gene Ther.* **4,** 797–807
37. Nordengren, J., Casslen, B., Gustavsson, B., Einarsdottir, M., and Willen, R. (1998) *Int. J. Cancer* **79,** 195–201
38. Im, D. S., Heise, C. E., Harding, M. A., George, S. R., O'Dowd, B. F., Theodorescu, D., and Lynch, K. R. (2000) *Mol. Pharmacol.* **57,** 753–759
39. Kingsbury, M. A., Rehen, S. K., Contos, J. J., Higgins, C. M., and Chun, J. (2003) *Nat. Neurosci.* **6,** 1292–1299
40. Fukushima, N., Ishii, I., Habara, Y., Allen, C. B., and Chun, J. (2002) *Mol. Biol. Cell* **13,** 2692–2705
41. Ohta, H., Sato, K., Murata, N., Damirin, A., Malchinkhuu, E., Kon, J., Kimura, T., Tobo, M., Yamazaki, Y., Watanabe, T., Yagi, M., Sato, M., Suzuki, R., Murooka, H., Sakai, T., Nishitoba, T., Im, D. S., Nochi, H., Tamoto, K., Tomura, H., and Okajima, F. (2003) *Mol. Pharmacol.* **64,** 994–1005
42. Sanchez, T., and Hla, T. (2004) *J. Cell. Biochem.* **92,** 913–922
43. Toman, R. E., and Spiegel, S. (2002) *Neurochem. Res.* **27,** 619–627
44. Allende, M. L., and Proia, R. L. (2002) *Biochim. Biophys. Acta* **1582,** 222–227
45. Gardell, S. E., Dubin, A. E., and Chun, J. (2006) *Trends Mol. Med.* **12,** 65–75
46. Chun, J., and Rosen, H. (2006) *Curr. Pharm. Des.* **12,** 161–171